Published in final edited form as:

Neurobiol Aging. 2020 April ; 88: 42–50. doi:10.1016/j.neurobiolaging.2019.12.004.

Trajectory of Lobar Atrophy in Asymptomatic and Symptomatic *GRN* Mutation Carriers: a Longitudinal MRI Study

*Corresponding Author: Kejal Kantarci, MD, MS., Department of Radiology, Mayo Clinic, 200 First Street SW, Rochester, MN 55905, Phone: 507-284 9770, Fax: 507-284 9778, kantarci.kejal@mayo.edu.

Verification

We verify that the data contained in the manuscript being submitted have not been previously published, have not been submitted elsewhere and will not be submitted elsewhere while under consideration at *Neurobiology of Aging*. All authors have reviewed the contents of the manuscript being submitted, approve of its contents and validate the accuracy of the data.

Disclosure Statement

Chen Q – reports no competing interests

Boeve B - has served as an investigator for clinical trials sponsored by GE Healthcare and Axovant. He receives royalties from the publication of a book entitled Behavioral Neurology Of Dementia (Cambridge Medicine, 2009, 2017). He serves on the Scientific Advisory Board of the Tau Consortium. He receives research support from NIH, the Mayo Clinic Dorothy and Harry T. Mangurian Jr. Lewy Body Dementia Program and the Little Family Foundation.

Senjem M - reports no competing interests

Tosakulwong N- reports no competing interests

Lesnick T- reports no competing interests

Brushaber D - reports no competing interests

Dheel C - reports no competing interests Fields J - receives research support from NIH.

Forsberg L - receives research support from NIH.

Gavrilova R - receives research support from NIH.

Gearhart D - reports no competing interests

Graff-Radford J - receives research support from the NIH.

Graff-Radford N - receives royalties from UpToDate, has participated in multicenter therapy studies by sponsored by Biogen, TauRx, AbbVie, Novartis and Lilly. He receives receives research support from NIH.

Jack, CR, Jr. - consults for Eli Lilly and serves on an independent data monitoring board for Roche but he receives no personal compensation from any commercial entity. He receives research support from the NIH.

Jones D - receives research support from NIH and the Minnesota Partnership for Biotechnology and Medical Genomics.

Knopman D - serves on the DSMB of the DIAN-TU study, is a site PI for clinical trials sponsored by Biogen, Lilly and the University of Southern California, and is funded by NIH.

Kremers W - receives research funding from AstraZeneca, Biogen, Roche, DOD and NIH.

Lapid M - reports no competing interests

Rademakers R - receives research funding from NIH and the Bluefield Project to Cure Frontotemporal Dementia.

Ramos EM - reports no disclosures relevant to the manuscript.

Ramos E - reports no competing interests

Syrjanen J - reports no competing interests

Boxer A - receives research support from NIH, the Tau Research Consortium, the Association for Frontotemporal Degeneration, Bluefield Project to Cure Frontotemporal Dementia, Corticobasal Degeneration Solutions, the Alzheimer's Drug Discovery Foundation and the Alzheimer's Association. He has served as a consultant for Aeton, Abbvie, Alector, Amgen, Arkuda, Ionis, Iperian, Janssen, Merck, Novartis, Samumed, Toyama and UCB, and received research support from Avid, Biogen, BMS, C2N, Cortice, Eli Lilly, Forum, Genentech, Janssen, Novartis, Pfizer, Roche and TauRx.

Rosen H - has received research support from Biogen Pharmaceuticals, has consulting agreements with Wave Neuroscience and Ionis Pharmaceuticals, and receives research support from NIH.

Wszolek Z - supported by the NIH, Mayo Clinic Center for Regenerative Medicine, the gift from Carl Edward Bolch, Jr., and Susan Bass Bolch, The Sol Goldman Charitable Trust, and Donald G. and Jodi P. Heeringa. He has also received grant funding support from Allergan, Inc. (educational grant), and Abbvie (medication trials).

Kantarci K - served on the Data Safety Monitoring Board for Takeda Global Research & Development Center, Inc.; data monitoring boards of Pfizer and Janssen Alzheimer Immunotherapy; research support from the Avid Radiopharmaceuticals, Eli Lilly, the Alzheimer's Drug Discovery Foundation and NIH.

Qin Chen, M.D. Ph.D[1,2], **Bradley F. Boeve, M.D.**[3,7], **Matthew Senjem**[2], **Nirubol Tosakulwong**[4], **Timothy Lesnick, MS**[4], **Danielle Brushaber**[4,7], **Christina Dheel**[3,7], **Julie Fields, Ph.D. L.P**[5], **Leah Forsberg, Ph.D**[3,7], **Ralitza Gavrilova, M.D.**[6], **Debra Gearhart**[3,7], **Jonathan Graff-Radford, M.D.**[3,7], **Neill Graff-Radford, M.D.**[8], **Clifford R Jack Jr., M.D.**[2,7], **David Jones, M.D**[3,7], **David Knopman, M.D.**[3,7], **Walter K. Kremers, Ph.D.**[4], **Maria Lapid, M.D.**[5], **Rosa Rademakers, Ph.D.**[7,9], **Eliana Marisa Ramos, Ph.D.**[10], **Jeremy Syrjanen**[4], **Adam L. Boxer, M.D. Ph.D**[11], **Howie Rosen, M.D.**[11], **Zbigniew K. Wszolek, M.D.**[8], **Kejal Kantarci, M.D. M.S.**[2,7,*]

[1]Department of Neurology, West China Hospital of Sichuan University, Chengdu, Sichuan, China

[2]Department of Radiology, Mayo Clinic, Rochester, Minnesota

[3]Department of Neurology, Mayo Clinic, Rochester, Minnesota

[4]Department of Health Sciences Research, Mayo Clinic, Rochester, Minnesota

[5]Department of Psychology and Psychiatry, Mayo Clinic, Rochester, Minnesota

[6]Department of Clinical Genomic and Neurology, Mayo Clinic, Rochester, Minnesota

[7]Alzheimer's Disease Research Center, Mayo Clinic, Rochester, Minnesota

[8]Department of Neurology, Mayo Clinic, Jacksonville, Florida

[9]Department of Neuroscience, Mayo Clinic, Jacksonville, Florida

[10]Department of Psychiatry, David Geffen School of Medicine, University of California Los Angeles, Los Angeles, California

[11]Memory and Aging Center, University of California San Francisco, San Francisco

Abstract

Loss-of-function mutations in the progranulin gene (*GRN*) are one of the major causes of familial frontotemporal lobar degeneration (FTLD). Our objective was to determine the rates and trajectories of lobar cortical atrophy from longitudinal structural MRI in both asymptomatic and symptomatic *GRN* mutation carriers. Individuals in this study were from the ADRC and LEFFTDS studies at the Mayo Clinic. We identified 13 *GRN* mutation carriers (8 asymptomatic, 5 symptomatic) and non-carriers (n=10) who had at least 2 serial T1-weighted structural MRIs and were followed annually with a median of 3 years (range 1.0 to 9.8 years). Longitudinal changes in lobar cortical volume were analyzed using the tensor-based morphometry with symmetric normalization (TBM-SyN) algorithm. Linear mixed effect models were used to model cortical volume change over time among 3 groups. The annual rates of frontal ($p<0.05$) and parietal ($p<0.01$) lobe cortical atrophy were higher in asymptomatic *GRN* mutation carriers than non-carriers. The symptomatic *GRN* mutation carriers also had increased rates of atrophy in the frontal ($p<0.01$) and parietal lobe ($p<0.01$) cortices than non-carriers. In addition, greater rates of cortical atrophy were observed in the temporal lobe cortices of symptomatic *GRN* mutation carriers than non-carriers ($p<0.001$). We found that a decline in frontal and parietal lobar cortical volume occurs in asymptomatic *GRN* mutation carriers and continues in the symptomatic *GRN* mutation carriers, while an increased rate of temporal lobe cortical atrophy is observed only in symptomatic *GRN* mutation carriers. This sequential pattern of cortical involvement in *GRN* mutation carriers has

important implications for utilizing imaging biomarkers of neurodegeneration as an outcome measure in potential treatment trials involving *GRN* mutation carriers.

Keywords

magnetic resonance image; *GRN*; asymptomatic; frontotemporal dementia; longitudinal

1. Introduction

About 30%−50% of patients with frontotemporal lobar degeneration (FTLD) have a family history with an autosomal dominant pattern of inheritance (Rohrer and Warren, 2011). Loss-of-function mutations in the progranulin gene (*GRN*) were first identified in 2006 as one of the major causes of familial FTLD (Baker et al., 2006; Cruts et al., 2006). To date, more than 70 different pathogenetic *GRN* mutations have been identified (http://www.molgen.ua.ac.be/FTDmutations). The *GRN* mutations result in a loss of progranulin levels through haploinsufficiency which lead to intraneuronal aggregation of TDP-43 protein (Pottier et al., 2016), with the most frequent clinical phenotypes being behavioral variant frontotemporal dementia (bvFTD), primary progressive aphasia (PPA) and corticobasal syndrome (CBS) (Beck et al., 2008; Kelley et al., 2009). Families characterized by the presence of *GRN* mutations are being investigated for early neurodegenerative changes and to identify biomarkers for tracking disease progression in preparation for potential disease modifying therapies.

Previous structural magnetic resonance imaging (MRI) studies have captured an asymmetric and widespread pattern of brain atrophy in FTLD patients with *GRN* mutations, predominantly involving the frontal, posterior temporal and inferior parietal cortices (Beck et al., 2008; Cash et al., 2018; Premi et al., 2016; Rohrer et al., 2010; Whitwell et al., 2009; Whitwell et al., 2012; Whitwell et al., 2011). However, the structural MRI studies in asymptomatic *GRN* mutation carriers were inconsistent (Caroppo et al., 2015; Olm et al., 2018; Pievani et al., 2014; Rohrer et al., 2008). Most found no significant grey matter volume differences between asymptomatic *GRN* mutation carriers and controls in cross-sectional and longitudinal analysis(Borroni et al., 2012; Borroni et al., 2008; Dopper et al., 2014; Panman et al., 2019; Popuri et al., 2018). On the contrary, a recent study reported extensive grey matter volume loss mainly in the temporal and frontal lobes after combining 5 microtubule-associated protein tau (*MAPT)* mutation and 3 *GRN* mutation carriers who later progressed to the symptomatic state, but found no longitudinal grey matter volume loss in asymptomatic *MAPT* and *GRN* mutation carriers who did not progress compared with non-carriers, indicating that accelerated grey matter atrophy occurs right before symptom onset (Jiskoot et al., 2019). However, the pattern of progression of atrophy on longitudinal MRI in asymptomatic *GRN* mutation carriers is not established. Furthermore, the ability to capture longitudinal structural MRI changes may depend on the methodology used in quantifying regional brain volume changes.

In this study, our objective was to investigate the rates and trajectories of lobar cortical atrophy from longitudinal structural MRI in both asymptomatic and symptomatic *GRN* mutation carriers.

2. Methods

2.1. Participants

Individuals in this study were participants enrolled in the Mayo Clinic Alzheimer's Disease Research Center (ADRC) and the Longitudinal Evaluation of Familial Frontotemporal Dementia Subjects (LEFFTDS) studies at the Mayo Clinic site. Mayo Clinic ADRC is one of Alzheimer's disease centers in the U.S. funded by the National Institute on Aging. Patients and families with a history of FTLD and other dementias are referred to ADRC through the behavioral neurology clinical practice. LEFFTDS is a multi-site study investigating the biomarkers of disease progression in familial FTLD mutation carriers that began in 2014. The current study included participants who screened positive for a mutation in *GRN* and had been followed between June 2008 and June 2018 at Mayo Clinic. We identified 13 *GRN* mutation carriers (8 asymptomatic, 5 symptomatic) and 10 non-carriers from 7 families who had at least 2 serial T1-weighted structural MRIs and who were followed annually with a median follow-up time of 3 years (range 1 to 9.8 years). A total of 83 MRI scans were included (Supplemental Table 1).

2.2. Baseline characteristics

Among the 13 *GRN* mutation carriers, 8 participants had no clinical symptoms at baseline and a Clinical Dementia Rating® Staging Instrument plus National Alzheimer's Coordinating Center Frontotemporal Lobar Degeneration Module Sum of the Boxes score (CDR® plus NACC FTLD-SB) (Knopman et al., 2008) of 0, which we refer to as asymptomatic *GRN* mutation carriers. At baseline, symptomatic *GRN* mutation carriers (n=5) had a median CDR® plus NACC FTLD -SB score of 2.5 including: 1 participant with a primary diagnosis of mild cognitive impairment (MCI), 1 with MCI at baseline who later progressed to bvFTD, 1 with bvFTD, 1 with mixed PPA and CBS, and 1 with atypical FTLD with right parietal lobe syndrome. The mutations identified in these symptomatic *GRN* mutation carriers were as follows: c.154delA, p.T52Hfs*2 (n=2), c.910_911dupTG, p.W304Cfs*58 (n=1), c.882T>G, p.Y294* (n=1) and c.1535delC, p.P512Lfs*5 (n=1). The median age of symptom onset was 62 years with a range of 58 – 67 years, and the median follow-up interval was 2.2 years (range 1–3.4 years) for these patients. Healthy first-degree relatives of the patients who were mutation non-carriers were included as the control group after DNA screening (n=10).

All participants were followed prospectively with annual clinical examinations at the time of MRI examinations, including a medical history review, mental status examination, a neurological examination by a clinician with FTLD expertise and a neuropsychological examination. The behavioral neurologists (BB, JGR, NGR, DJ, or DK) who examined the participants were blinded to the mutation status. None of the participants had structural lesions that could cause cognitive impairment or dementia, such as cortical infarction,

subdural hematoma, or tumor, or had concurrent illness that would interfere with cognitive function other than FTLD on baseline and follow-up examinations.

2.3. Longitudinal follow-up

During follow up, 6 asymptomatic *GRN* mutation carriers remained as having no cognitive/behavioral/motor changes, which was corroborated by their informants and had a MoCA score of 30 throughout, with a median follow-up interval of 4.2 years (range 1.0–7.5 years). The remaining 2 participants progressed from the asymptomatic to symptomatic stage. Both participants were classified as MCI at the time of conversion, with one participant later developing features of bvFTD, and the other participant later developing features of mixed PPA and bvFTD (Figure 1). The scans after conversion from these 2 participants were not involved in the asymptomatic *GRN* mutation carriers for group analysis.

All symptomatic *GRN* mutation carriers described in this report have undergone clinical genetic testing. Therefore, they and their proxies, as well as the examining neurologist, were aware of their mutation status. Most of the asymptomatic mutation carriers involved in this study have not undergone clinical genetic testing, and therefore are not aware of their mutation status, nor are the examining neurologists. Details regarding each person have intentionally been excluded to maintain confidentiality.

Informed consent was obtained from all participants for participation in the studies, and after the two converters developed dementia, written assent was also obtained by their proxies. All procedures were approved by the Mayo Institutional Review Board.

2.4. MRI acquisition and process

All participants underwent annual volumetric MRI at 3T using an 8-channel phased array head coil (GE Healthcare, Milwaukee, WI). A 3D high-resolution T1-weighted magnetization-prepared rapid acquisition gradient echo (MPRAGE) was performed at each time-point using the following parameters: repetition time/echo time/inversion time = 2300/3/900 msec, flip angle 8 degrees, in-plane resolution of 1.0 mm.

2.5. TBM-SyN Analysis

Baseline and annual changes in cortical volume were estimated for each participant. We applied a fully automated in-house developed image-processing pipeline for the region-level analysis, using tensor-based morphometry with symmetric normalization (TBM-SyN) to compute the baseline lobar cortical volumes and changes over time in each participant (Cash et al., 2015). For each individual, all of their T1 structural MRI scans were iteratively co-registered to a mean image using SPM co-registration software(Ashburner and Friston, 2005) (www.fil.ion.ucl.ac.uk/spm) with a 6 degrees-of-freedom (6-DOF) for rigid-body co-registration of each image to the subject's baseline image, followed by 9-DOF rigid body registration of each time point image to the mean image. Then we normalized image intensity histograms across each participant's time series of images by using an in-house developed differential bias correction algorithm(Avants et al., 2008). The SyN diffeomorphic registration algorithm from ANTs software(Avants et al., 2008) was used to compute deformations between each pair of images, running the deformations explicitly in each

direction, producing the Jacobian determinant images and the "annualized" log of the Jacobian determinant from the deformation in each direction, to be parcellated into lobar regions of interest (ROIs) later. The voxel values of the Jacobian determinant image represent the expansion or contraction of each voxel over time, and those of the annualized log Jacobian determinant image can be thought of as analogous to an annualized percent change at each voxel. The SyN deformations were applied in each direction, respectively to the original bias corrected late and early images, to get the early image warped to the late, and the late image warped to the early image, and average them with their respective originals, resulting in a "synthetic late image" and a "synthetic early image". Then, we segmented the synthetic early and late images into gray matter, white matter and cerebrospinal fluid classes using the SPM unified segmentation algorithm, with our in-house developed custom template and tissue priors (Vemuri et al., 2008). The discrete cosine spatial normalization parameters from the SPM unified segmentation step were used to transform the in-house modified Automated Anatomical Labeling (AAL) atlas that included the frontal, temporal, parietal and occipital ROI labels from template space to the synthetic early and late image spaces, respectively (Tzourio-Mazoyer et al., 2002). The resulting subject-space atlas was used to assess baseline GM volume from the first MRI scan, and the follow-up GM volumes for each image pair by summing the GM probabilities within each ROI, as well as to extract mean values of the annualized log of the Jacobian determinant from each ROI.

2.6 Voxel-based Analysis

To assess the rates of atrophy at the voxel level, the first and last image were used for each participant. The TBM-SyN steps were run as detailed above to produce an image of the annualized log of the Jacobian determinant over the largest possible time interval for each participant, smoothed with a 6 mm full-width at half maximum (FWHM) Gaussian smoothing kernel. The smoothed annualized log Jacobian determinant images were then entered into a multiple regression analysis in SPM, with groups encoded as categorical variables, and age included as an additional covariate. Correction for multiple comparisons was applied with false discovery rate (FDR).

2.7 Genetic analysis

All participants were part of known *GRN* families. We specifically sequenced the exon harboring the known *GRN* gene mutation observed in their families using the previously published protocol (Baker et al., 2006; Gass et al., 2006). Exons 0–12 and the 3′ untranslated region of the *GRN* gene were amplified by polymerase chain reaction (PCR) assay. The PCR amplicons were purified using the Multiscreen system (Millipore, Billerica, MA) and then sequenced in both directions using Big Dye chemistry following the manufacturer's protocol (Applied Biosystems, Foster City, CA). Sequence products were purified using the Montage system (Millipore) before being run on an Applied Biosystem 3730 DNA Analyzer. Sequence data were analyzed using either SeqScape (Applied Biosystems) or Sequencher software (Gene Codes, Ann Arbor, MI). Furthermore, sequencing is also performed to detect variants in the following genes *MAPT*, *C9orf72*, *TARDBP*, *PSEN1*, *PSEN2* and *APP* according to the LEFFTDS protocol.

2.8 Statistical analysis

Baseline characteristics were described with means, standard deviations, counts and proportions. Baseline characteristics were compared among asymptomatic, symptomatic *GRN* mutation carriers and non-carriers using logistic mixed effect models for sex and linear mixed effect models for the other variables. These models were adjusted for age at MRI where appropriate, and accounted for within-family correlations through inclusion of family as a random effect. Tukey contrasts based on the mixed models were used for pair-wise comparisons for continuous variables. For the analysis of baseline GM volume, linear mixed models were used after adjusting for age at MRI and log-transformed total intra-cranial volume (TIV), also accounting for within-family correlations, followed by Tukey contrasts for pair-wise comparisons.

The lobar cortical volumes (scaled to cm^3) were modeled to estimate rate of volume loss per year using linear mixed effect models with random subject-specific intercepts and slopes, while accounting for within-family correlations through a random family effect. We coded group (non-carriers, asymptomatic, or symptomatic) using dummy variables with non-carrier as the reference, and included two-way interactions for group × age at MRI scan. Assessments of voxel level results were corrected for multiple comparisons by requiring the corrected false discovery rate (FDR) to be <0.05.

3. Results

3.1 Participant baseline characteristics

Characteristics of participants in each group are listed in Table 1. There were no differences among the 3 groups at baseline based on sex, age and education. As expected, symptomatic *GRN* mutation carriers had lower MoCA scores and higher scores in CDR® plus NACC FTLD-SB than asymptomatic *GRN* mutation carriers ($p<0.001$) and non-carriers ($p<0.001$). In asymptomatic *GRN* mutation carriers, the lobar cortical volumes were lower in frontal ($p=0.04$) and occipital ($p=0.04$) lobes compared with non-carriers at baseline. In symptomatic *GRN* mutation carriers, the baseline lobar cortical volumes were lower in the frontal ($p<0.001$), parietal ($p=0.003$) and occipital ($p<0.001$) lobes than non-carriers, also lower in frontal ($p=0.02$) and occipital ($p=0.04$) lobes compared to asymptomatic *GRN* mutation carriers (Supplemental Table 2). No difference was observed in the temporal lobe volume at baseline among the 3 groups.

3.2 Lobar rates of atrophy

The trajectories of change in lobar cortical volumes are shown in the top row of Figure 2. Hemispheric volumes were averaged because on average there were no differences in left and right lobar cortical volume changes in the *GRN* mutation carriers ($p>0.05$). The results of linear mixed effects models are summarized in Table 2, and predicted lines for the 50–70 age range are shown in the bottom row of Figure 2. The estimated rates of lobar atrophy for each group were summarized in Supplemental Table 3. Group× age at MRI scan interactions indicated that in asymptomatic *GRN* mutation carriers, lobar rates of atrophy were greater in the frontal (-0.59 cm^3/year, $p<0.05$) and parietal lobes (-0.30 cm^3/year, $p<0.01$) compared to non-carriers. Furthermore, symptomatic *GRN* mutation carriers showed greatest annual

rate of atrophy in the temporal lobe (−1.55 cm^3/year, p <0.001), followed by the frontal (−1.44 cm^3/year, p <0.01) and parietal (−0.71 cm^3/year, p <0.01) lobes compared to non-carriers. Compared with asymptomatic *GRN* mutation carriers, symptomatic *GRN* mutation carriers also showed the greatest annual rate of lobar cortical atrophy in the temporal lobe (p<0.001), followed by frontal (p<0.05) and parietal lobes (p<0.05) (Supplemental Table 4). As a potential biomarker, which can be used in future clinical trials, we combined the frontal and parietal lobe volume as a composite frontal-parietal volume. The annual change for the composite volume of frontal and parietal lobes show the most robust change in the asymptomatic (−0.90 cm^3/year, p <0.01) as well as symptomatic phases (−2.15 cm^3/year, p <0.001) compared to non-carriers. There was no difference in the estimated annual rate of occipital lobe cortical volume change among the 3 groups.

3.3 Voxel-level analysis

Voxel based analysis showed that the annualized rate of atrophy was localized to the bilateral frontal, temporal and parietal lobes in symptomatic *GRN* mutation carriers compared to non-carriers (corrected FDR <0.05) (Figure 3). There was some asymmetry in atrophy mainly involving the left hemisphere in the prefrontal cortex and inferior frontal and temporal lobe cortices after comparison the left and right hemisphere of the thresholded T-map (Supplemental Figure 3). No difference in voxel based analysis was observed in annualized rates of atrophy comparing asymptomatic *GRN* mutation carriers and the other 2 groups (corrected for FDR<0.05).

4. Discussion

In this study, we investigated the regional rates of cortical atrophy in *GRN* mutation carriers during both asymptomatic and symptomatic stages by using multiple serial MRI scans and mixed effects modeling. In asymptomatic *GRN* mutation carriers, lower cortical lobar volume was observed in frontal and occipital lobes at baseline when compared to non-carriers. However, our longitudinal data showed that the trajectories of lobar cortical atrophy were greater in the frontal and parietal lobes in asymptomatic *GRN* mutation carriers compared to non-carriers as they aged. The symptomatic *GRN* mutation carriers, in whom cortical atrophy was already present, showed the fastest rate of cortical atrophy in the temporal lobe, followed by the frontal and parietal lobes compared to non-carriers. Our cross-sectional and longitudinal findings revealed a sequential pattern of lobar cortical atrophy in *GRN* mutation carriers throughout the disease course in this cohort, indicating that the frontal and parietal lobe cortical volume began declining during the asymptomatic stage, with an acceleration of the rates of cortical atrophy especially in temporal lobe in the symptomatic stage. Combining frontal and parietal lobe volumes into a composite volume appears to show the most robust change in the asymptomatic as well as symptomatic phases.

In the current study, the frontal and parietal lobe cortical volume decline started in *GRN* mutation carriers as early as the asymptomatic stage, and became more atrophic as the disease progressed in the symptomatic stage. Especially, the frontal lobe volumes are already lower than non-carriers at baseline, suggesting the frontal lobe might be affected even early. In keeping with the cognitive and behavioral features typically observed in FTLD, the

progressive pattern of fronto-parietal cortical atrophy is consistent with the fronto-parietal-temporal network involvement in symptomatic *GRN* mutation carriers (Fumagalli et al., 2018; Rohrer et al., 2010; Whitwell et al., 2015; Whitwell et al., 2009). The early involvement of fronto-parietal lobes was also found in a longitudinal arterial spin labeling (ASL) study that demonstrated early hypoperfusion in frontal and parietal lobes in asymptomatic *GRN* mutation carriers (Dopper et al., 2016). Similarly, reduced cortical thickness in the orbitofrontal cortex, middle frontal and precentral gyri was reported in asymptomatic *GRN* carriers (Pievani et al., 2014). The involvement of frontal and parietal hubs have also been shown in previous works on functional connectivity in *GRN* mutation carriers as early as the presymptomatic phase (Dopper et al., 2014; Premi et al., 2014a). Although most of prior structural MRI studies found no difference in grey matter volume between asymptomatic *GRN* mutation carriers and controls on cross-sectional and longitudinal studies (Borroni et al., 2012; Borroni et al., 2008; Panman et al., 2019; Popuri et al., 2018), some recent studies reported a grey matter atrophy pattern involving frontal, parietal and temporal lobes, which did not survive correction for multiple comparisons (Cash et al., 2018; Olm et al., 2018). Compared with other structural imaging techniques (eg. voxel based morphometry and cortical thickness analysis) previously studied in presymptomatic carriers of *GRN* mutations, longitudinal design with multiple time points can demonstrate change over time and may be superior to the cross-sectional analysis (Cash et al., 2018) or independent VBM analysis on two time points (Panman et al., 2019). Our data confirm and extend those findings demonstrating that progressive frontal and parietal lobe cortical atrophy occurs early in the asymptomatic stage in *GRN* mutation carriers, suggesting the characteristic progression pattern of network involvement.

Our data demonstrate accelerated rates of atrophy in the temporal lobes of symptomatic *GRN* mutation carriers during follow-up compared to non-carriers. However, the rates of cortical atrophy in the temporal lobe were not different between asymptomatic *GRN* mutation carriers and non-carriers. Thus, the temporal lobe cortical atrophy occurred after frontal and parietal lobe involvement. Similarly, Rohrer et al. evaluated a *GRN* mutation carrier longitudinally and noted that the left temporal and fusiform gyri were particularly affected at the approximate time of clinical onset (Rohrer et al., 2008). Thus, the temporal lobe may be affected later during the transition period from asymptomatic to symptomatic status in *GRN* mutation carriers. On the contrary, temporal lobe hypometabolism was reported to be the earliest finding in asymptomatic *GRN* mutation carriers predominantly involving the left lateral temporal lobe without any structural changes (Caroppo et al., 2015). These inconsistencies might be due to the age at examination, the proximity to clinical symptom onset, the sample size of *GRN* mutation carriers, the phenotypes and associated lobar cortical atrophy changes, and statistical methodology. Taken together with our findings, the temporal progression of lobar atrophy may follow a sequential pattern in *GRN* mutation carriers. Greater rates of fronto-parietal cortical atrophy occur during the earliest asymptomatic stage. In the symptomatic stage, the atrophy continues in the fronto-parietal lobe cortices, but also accelerates in the temporal lobes as the disease progresses with the onset of symptoms. Future studies will need to investigate this sequential pattern of regional atrophy rates in a larger cohort of converters with a longitudinal study design.

Voxel based analysis revealed widespread increased cortical atrophy rates involving bilateral frontal, temporal and parietal lobes in symptomatic *GRN* mutation carriers, consistent with previous reports (Beck et al., 2008; Rohrer et al., 2010; Whitwell et al., 2009). Our results appeared to be more symmetric, while some left predominant asymmetry was indeed observed, especially in the prefrontal cortex and inferior frontal and temporal cortices. Asymmetric atrophy is a common finding in *GRN* mutation carriers with both left and right asymmetry observed even in the same family (Rohrer et al., 2010; Whitwell et al., 2012). Although the underlying cause for this asymmetry remains unclear, asymmetric cortical atrophy was reported 5 years before expected symptom onset in asymptomatic *GRN* mutation carriers (Rohrer et al., 2015). However, symmetric rates of atrophy were also reported in FTLD patients with *GRN* mutations in a longitudinal study (Whitwell et al., 2015). One possible explanation for the discrepancy is that asymmetry in atrophy rates may be more apparent early in the disease stage, becoming more symmetric over time (Whitwell et al., 2015), or as noted above, the specific phenotype and associated lobar cortical atrophy changes, also may be related with the different sensitivity and specificity of the analysis methods.

Consistent with prior voxel-based analysis studies, we found no difference in voxel-based analysis of annualized rates of atrophy between asymptomatic *GRN* mutation carriers and non-carriers. This may be because of larger effect sizes and corrections for multiple comparisons are needed to detect differences in annualized rates of atrophy between groups compared to the rates of atrophy in the ROIs from five lobes we studied. Many studies have shown that mutations in *GRN* are associated with heterogeneity during the early phase of clinical presentation as well as variability in age of onset.(Ghidoni et al., 2012; van Swieten and Heutink, 2008) Furthermore, different time windows during the disease course may have influenced the variability in findings in regional atrophy rates and laterality across individuals. This may in part explain the inconsistent findings of grey matter atrophy in asymptomatic *GRN* mutation carriers in cross-sectional studies. In the current study, we measured the rate of change in lobar cortical volume in both hemispheres across time without considering any significant asymmetry of focal change, since on average, we did not observe laterality across all *GRN* mutation carriers. However, it is important to note that laterality occurs at various stages of neurodegenerative disease progression, which may increase the variability in atrophy rates in individual *GRN* mutation carriers. Thus the findings in our sample may not be fully representative of all *GRN* mutation carriers.

The strength of our study was the large number of serial MRIs collected in each participant over up to10 years. However, the relatively small number of participants in each clinical group was still a limitation. The family-based design in current study had some advantages such as. control of unmeasured environmental factors, enrichment of GRN mutation frequency and restrictions because the findings are only generalizable to familial FTLD, not to general population. Although age is not significantly different among groups, symptomatic GRN mutation carriers are older than non-carriers. An age-matched group of non-carriers for symptomatic GRN mutation carriers are needed in future studies. Furthermore, while we included all available scans for each participant, the follow-up interval varied. Annualizing the rates of change normalizes the variations in follow-up intervals by assuming linearity in the change in cortical volume over time. However, a

limitation of this approach is that rates of change may vary across disease stages. Future studies with larger cohorts of asymptomatic *GRN* mutation carriers with a relatively short follow-up interval longitudinal design for tracking the trajectory of cortical atrophy during conversion from the asymptomatic to the symptomatic state would be needed. Since there is heterogeneity in age of symptom onset across different *GRN* mutations/families and within the same family, considering the effect from other genetic and environmental factors, such as TMEM106B polymorphism (Premi et al., 2014b; Premi et al., 2017), on neurodegeneration may help to better understand the heterogeneity of disease progression in *GRN* mutation carriers.

5. Conclusion

In summary, our data in this cohort indicate a sequential pattern of regional cortical atrophy rates involving the frontal and parietal lobe cortices early during the asymptomatic stage, followed by the temporal lobe cortex after symptom onset in *GRN* mutation carriers. Our findings support the utility of using longitudinal change in regional cortical volumes, especially the composite of fronto-parietal lobes, for monitoring the neurodegenerative disease progression in *GRN* mutation carriers starting from the asymptomatic stage, potentially as an outcome measure in future clinical trials.

Supplementary Material

Refer to Web version on PubMed Central for supplementary material.

Acknowledgements

We extend our appreciation to the staff of all centers, and particularly to our patients and their families for their participation in this protocol.

Study Funding: This study is funded by U01 AG045390, U54 NS092089, U24 AG021886, U01 AG016976, R01 AG40042, and the Bluefield Project. The funding sources had no role in study design, collection, analysis, interpretation, or decision to submit this paper. The corresponding author had full access to all the data in the study and had final responsibility for the decision to submit for publication.

References

Ashburner J, Friston KJ, 2005 Unified segmentation. Neuroimage 26(3), 839–851. [PubMed: 15955494]

Avants BB, Epstein CL, Grossman M, Gee JC, 2008 Symmetric diffeomorphic image registration with cross-correlation: evaluating automated labeling of elderly and neurodegenerative brain. Med Image Anal 12(1), 26–41. [PubMed: 17659998]

Baker M, Mackenzie IR, Pickering-Brown SM, Gass J, Rademakers R, Lindholm C, Snowden J, Adamson J, Sadovnick AD, Rollinson S, Cannon A, Dwosh E, Neary D, Melquist S, Richardson A, Dickson D, Berger Z, Eriksen J, Robinson T, Zehr C, Dickey CA, Crook R, McGowan E, Mann D, Boeve B, Feldman H, Hutton M, 2006 Mutations in progranulin cause tau-negative frontotemporal dementia linked to chromosome 17. Nature 442(7105), 916–919. [PubMed: 16862116]

Beck J, Rohrer JD, Campbell T, Isaacs A, Morrison KE, Goodall EF, Warrington EK, Stevens J, Revesz T, Holton J, Al-Sarraj S, King A, Scahill R, Warren JD, Fox NC, Rossor MN, Collinge J, Mead S, 2008 A distinct clinical, neuropsychological and radiological phenotype is associated with progranulin gene mutations in a large UK series. Brain 131(Pt 3), 706–720. [PubMed: 18234697]

Borroni B, Alberici A, Cercignani M, Premi E, Serra L, Cerini C, Cosseddu M, Pettenati C, Turla M, Archetti S, Gasparotti R, Caltagirone C, Padovani A, Bozzali M, 2012 Granulin mutation drives

brain damage and reorganization from preclinical to symptomatic FTLD. Neurobiol Aging 33(10), 2506–2520. [PubMed: 22130207]

Borroni B, Alberici A, Premi E, Archetti S, Garibotto V, Agosti C, Gasparotti R, Di Luca M, Perani D, Padovani A, 2008 Brain magnetic resonance imaging structural changes in a pedigree of asymptomatic progranulin mutation carriers. Rejuvenation Res 11(3), 585–595. [PubMed: 18593276]

Caroppo P, Habert MO, Durrleman S, Funkiewiez A, Perlbarg V, Hahn V, Bertin H, Gaubert M, Routier A, Hannequin D, Deramecourt V, Pasquier F, Rivaud-Pechoux S, Vercelletto M, Edouart G, Valabregue R, Lejeune P, Didic M, Corvol JC, Benali H, Lehericy S, Dubois B, Colliot O, Brice A, Le Ber I, Predict P.s.g., 2015 Lateral Temporal Lobe: An Early Imaging Marker of the Presymptomatic GRN Disease? J Alzheimers Dis 47(3), 751–759. [PubMed: 26401709]

Cash DM, Bocchetta M, Thomas DL, Dick KM, van Swieten JC, Borroni B, Galimberti D, Masellis M, Tartaglia MC, Rowe JB, Graff C, Tagliavini F, Frisoni GB, Laforce R Jr., Finger E, de Mendonca A, Sorbi S, Rossor MN, Ourselin S, Rohrer JD, Genetic Ftd Initiative G, 2018 Patterns of gray matter atrophy in genetic frontotemporal dementia: results from the GENFI study. Neurobiol Aging 62, 191–196. [PubMed: 29172163]

Cash DM, Frost C, Iheme LO, Unay D, Kandemir M, Fripp J, Salvado O, Bourgeat P, Reuter M, Fischl B, Lorenzi M, Frisoni GB, Pennec X, Pierson RK, Gunter JL, Senjem ML, Jack CR Jr., Guizard N, Fonov VS, Collins DL, Modat M, Cardoso MJ, Leung KK, Wang H, Das SR, Yushkevich PA, Malone IB, Fox NC, Schott JM, Ourselin S, 2015 Assessing atrophy measurement techniques in dementia: Results from the MIRIAD atrophy challenge. Neuroimage 123, 149–164. [PubMed: 26275383]

Cruts M, Gijselinck I, van der Zee J, Engelborghs S, Wils H, Pirici D, Rademakers R, Vandenberghe R, Dermaut B, Martin JJ, van Duijn C, Peeters K, Sciot R, Santens P, De Pooter T, Mattheijssens M, Van den Broeck M, Cuijt I, Vennekens K, De Deyn PP, Kumar-Singh S, Van Broeckhoven C, 2006 Null mutations in progranulin cause ubiquitin-positive frontotemporal dementia linked to chromosome 17q21. Nature 442(7105), 920–924. [PubMed: 16862115]

Dopper EG, Chalos V, Ghariq E, den Heijer T, Hafkemeijer A, Jiskoot LC, de Koning I, Seelaar H, van Minkelen R, van Osch MJ, Rombouts SA, van Swieten JC, 2016 Cerebral blood flow in presymptomatic MAPT and GRN mutation carriers: A longitudinal arterial spin labeling study. Neuroimage Clin 12, 460–465. [PubMed: 27625986]

Dopper EG, Rombouts SA, Jiskoot LC, den Heijer T, de Graaf JR, de Koning I, Hammerschlag AR, Seelaar H, Seeley WW, Veer IM, van Buchem MA, Rizzu P, van Swieten JC, 2014 Structural and functional brain connectivity in presymptomatic familial frontotemporal dementia. Neurology 83(2), e19–26. [PubMed: 25002573]

Fumagalli GG, Basilico P, Arighi A, Bocchetta M, Dick KM, Cash DM, Harding S, Mercurio M, Fenoglio C, Pietroboni AM, Ghezzi L, van Swieten J, Borroni B, de Mendonca A, Masellis M, Tartaglia MC, Rowe JB, Graff C, Tagliavini F, Frisoni GB, Laforce R Jr., Finger E, Sorbi S, Scarpini E, Rohrer JD, Galimberti D, Genetic FTDI, 2018 Distinct patterns of brain atrophy in Genetic Frontotemporal Dementia Initiative (GENFI) cohort revealed by visual rating scales. Alzheimers Res Ther 10(1), 46. [PubMed: 29793546]

Gass J, Cannon A, Mackenzie IR, Boeve B, Baker M, Adamson J, Crook R, Melquist S, Kuntz K, Petersen R, Josephs K, Pickering-Brown SM, Graff-Radford N, Uitti R, Dickson D, Wszolek Z, Gonzalez J, Beach TG, Bigio E, Johnson N, Weintraub S, Mesulam M, White CL 3rd, Woodruff B, Caselli R, Hsiung GY, Feldman H, Knopman D, Hutton M, Rademakers R, 2006 Mutations in progranulin are a major cause of ubiquitin-positive frontotemporal lobar degeneration. Hum Mol Genet 15(20), 2988–3001. [PubMed: 16950801]

Ghidoni R, Paterlini A, Albertini V, Binetti G, Benussi L, 2012 Losing protein in the brain: the case of progranulin. Brain Res 1476, 172–182. [PubMed: 22348647]

Jiskoot LC, Panman JL, Meeter LH, Dopper EGP, Donker Kaat L, Franzen S, van der Ende EL, van Minkelen R, Rombouts S, Papma JM, van Swieten JC, 2019 Longitudinal multimodal MRI as prognostic and diagnostic biomarker in presymptomatic familial frontotemporal dementia. Brain 142(1), 193–208. [PubMed: 30508042]

Kelley BJ, Haidar W, Boeve BF, Baker M, Graff-Radford NR, Krefft T, Frank AR, Jack CR Jr., Shiung M, Knopman DS, Josephs KA, Parashos SA, Rademakers R, Hutton M, Pickering-Brown S,

Adamson J, Kuntz KM, Dickson DW, Parisi JE, Smith GE, Ivnik RJ, Petersen RC, 2009 Prominent phenotypic variability associated with mutations in Progranulin. Neurobiol Aging 30(5), 739–751. [PubMed: 17949857]

Knopman DS, Kramer JH, Boeve BF, Caselli RJ, Graff-Radford NR, Mendez MF, Miller BL, Mercaldo N, 2008 Development of methodology for conducting clinical trials in frontotemporal lobar degeneration. Brain 131(Pt 11), 2957–2968. [PubMed: 18829698]

Olm CA, McMillan CT, Irwin DJ, Van Deerlin VM, Cook PA, Gee JC, Grossman M, 2018 Longitudinal structural gray matter and white matter MRI changes in presymptomatic progranulin mutation carriers. Neuroimage Clin 19, 497–506. [PubMed: 29984158]

Panman JL, Jiskoot LC, Bouts M, Meeter LHH, van der Ende EL, Poos JM, Feis RA, Kievit AJA, van Minkelen R, Dopper EGP, Rombouts S, van Swieten JC, Papma JM, 2019 Gray and white matter changes in presymptomatic genetic frontotemporal dementia: a longitudinal MRI study. Neurobiol Aging 76, 115–124. [PubMed: 30711674]

Pievani M, Paternico D, Benussi L, Binetti G, Orlandini A, Cobelli M, Magnaldi S, Ghidoni R, Frisoni GB, 2014 Pattern of structural and functional brain abnormalities in asymptomatic granulin mutation carriers. Alzheimers Dement 10(5 Suppl), S354–S363 e351. [PubMed: 24418059]

Popuri K, Dowds E, Beg MF, Balachandar R, Bhalla M, Jacova C, Buller A, Slack P, Sengdy P, Rademakers R, Wittenberg D, Feldman HH, Mackenzie IR, Hsiung GR, 2018 Gray matter changes in asymptomatic C9orf72 and GRN mutation carriers. Neuroimage Clin 18, 591–598. [PubMed: 29845007]

Pottier C, Ravenscroft TA, Sanchez-Contreras M, Rademakers R, 2016 Genetics of FTLD: overview and what else we can expect from genetic studies. J Neurochem 138 Suppl 1, 32–53. [PubMed: 27009575]

Premi E, Cauda F, Costa T, Diano M, Gazzina S, Gualeni V, Alberici A, Archetti S, Magoni M, Gasparotti R, Padovani A, Borroni B, 2016 Looking for Neuroimaging Markers in Frontotemporal Lobar Degeneration Clinical Trials: A Multi-Voxel Pattern Analysis Study in Granulin Disease. J Alzheimers Dis 51(1), 249–262. [PubMed: 26836150]

Premi E, Cauda F, Gasparotti R, Diano M, Archetti S, Padovani A, Borroni B, 2014a Multimodal FMRI resting-state functional connectivity in granulin mutations: the case of fronto-parietal dementia. PLoS One 9(9), e106500.

Premi E, Formenti A, Gazzina S, Archetti S, Gasparotti R, Padovani A, Borroni B, 2014b Effect of TMEM106B polymorphism on functional network connectivity in asymptomatic GRN mutation carriers. JAMA Neurol 71(2), 216–221. [PubMed: 24343233]

Premi E, Grassi M, van Swieten J, Galimberti D, Graff C, Masellis M, Tartaglia C, Tagliavini F, Rowe JB, Laforce R Jr., Finger E, Frisoni GB, de Mendonca A, Sorbi S, Gazzina S, Cosseddu M, Archetti S, Gasparotti R, Manes M, Alberici A, Cardoso MJ, Bocchetta M, Cash DM, Ourselin S, Padovani A, Rohrer JD, Borroni B, Genetic FTDI, 2017 Cognitive reserve and TMEM106B genotype modulate brain damage in presymptomatic frontotemporal dementia: a GENFI study. Brain 140(6), 1784–1791. [PubMed: 28460069]

Rohrer JD, Nicholas JM, Cash DM, van Swieten J, Dopper E, Jiskoot L, van Minkelen R, Rombouts SA, Cardoso MJ, Clegg S, Espak M, Mead S, Thomas DL, De Vita E, Masellis M, Black SE, Freedman M, Keren R, MacIntosh BJ, Rogaeva E, Tang-Wai D, Tartaglia MC, Laforce R Jr., Tagliavini F, Tiraboschi P, Redaelli V, Prioni S, Grisoli M, Borroni B, Padovani A, Galimberti D, Scarpini E, Arighi A, Fumagalli G, Rowe JB, Coyle-Gilchrist I, Graff C, Fallstrom M, Jelic V, Stahlbom AK, Andersson C, Thonberg H, Lilius L, Frisoni GB, Pievani M, Bocchetta M, Benussi L, Ghidoni R, Finger E, Sorbi S, Nacmias B, Lombardi G, Polito C, Warren JD, Ourselin S, Fox NC, Rossor MN, Binetti G, 2015 Presymptomatic cognitive and neuroanatomical changes in genetic frontotemporal dementia in the Genetic Frontotemporal dementia Initiative (GENFI) study: a cross-sectional analysis. Lancet Neurol 14(3), 253–262. [PubMed: 25662776]

Rohrer JD, Ridgway GR, Modat M, Ourselin S, Mead S, Fox NC, Rossor MN, Warren JD, 2010 Distinct profiles of brain atrophy in frontotemporal lobar degeneration caused by progranulin and tau mutations. Neuroimage 53(3), 1070–1076. [PubMed: 20045477]

Rohrer JD, Warren JD, 2011 Phenotypic signatures of genetic frontotemporal dementia. Curr Opin Neurol 24(6), 542–549. [PubMed: 21986680]

Rohrer JD, Warren JD, Barnes J, Mead S, Beck J, Pepple T, Boyes R, Omar R, Collinge J, Stevens JM, Warrington EK, Rossor MN, Fox NC, 2008 Mapping the progression of progranulin-associated frontotemporal lobar degeneration. Nat Clin Pract Neurol 4(8), 455–460. [PubMed: 18648346]

Tzourio-Mazoyer N, Landeau B, Papathanassiou D, Crivello F, Etard O, Delcroix N, Mazoyer B, Joliot M, 2002 Automated anatomical labeling of activations in SPM using a macroscopic anatomical parcellation of the MNI MRI single-subject brain. Neuroimage 15(1), 273–289. [PubMed: 11771995]

van Swieten JC, Heutink P, 2008 Mutations in progranulin (GRN) within the spectrum of clinical and pathological phenotypes of frontotemporal dementia. Lancet Neurol 7(10), 965–974. [PubMed: 18771956]

Vemuri P, Whitwell JL, Kantarci K, Josephs KA, Parisi JE, Shiung MS, Knopman DS, Boeve BF, Petersen RC, Dickson DW, Jack CR Jr., 2008 Antemortem MRI based STructural Abnormality iNDex (STAND)-scores correlate with postmortem Braak neurofibrillary tangle stage. Neuroimage 42(2), 559–567. [PubMed: 18572417]

Whitwell JL, Boeve BF, Weigand SD, Senjem ML, Gunter JL, Baker MC, DeJesus-Hernandez M, Knopman DS, Wszolek ZK, Petersen RC, Rademakers R, Jack CR Jr., Josephs KA, 2015 Brain atrophy over time in genetic and sporadic frontotemporal dementia: a study of 198 serial magnetic resonance images. Eur J Neurol 22(5), 745–752. [PubMed: 25683866]

Whitwell JL, Jack CR Jr., Boeve BF, Senjem ML, Baker M, Rademakers R, Ivnik RJ, Knopman DS, Wszolek ZK, Petersen RC, Josephs KA, 2009 Voxel-based morphometry patterns of atrophy in FTLD with mutations in MAPT or PGRN. Neurology 72(9), 813–820. [PubMed: 19255408]

Whitwell JL, Weigand SD, Boeve BF, Senjem ML, Gunter JL, DeJesus-Hernandez M, Rutherford NJ, Baker M, Knopman DS, Wszolek ZK, Parisi JE, Dickson DW, Petersen RC, Rademakers R, Jack CR Jr., Josephs KA, 2012 Neuroimaging signatures of frontotemporal dementia genetics: C9ORF72, tau, progranulin and sporadics. Brain 135(Pt 3), 794–806. [PubMed: 22366795]

Whitwell JL, Weigand SD, Gunter JL, Boeve BF, Rademakers R, Baker M, Knopman DS, Wszolek ZK, Petersen RC, Jack CR Jr., Josephs KA, 2011 Trajectories of brain and hippocampal atrophy in FTD with mutations in MAPT or GRN. Neurology 77(4), 393–398. [PubMed: 21753165]

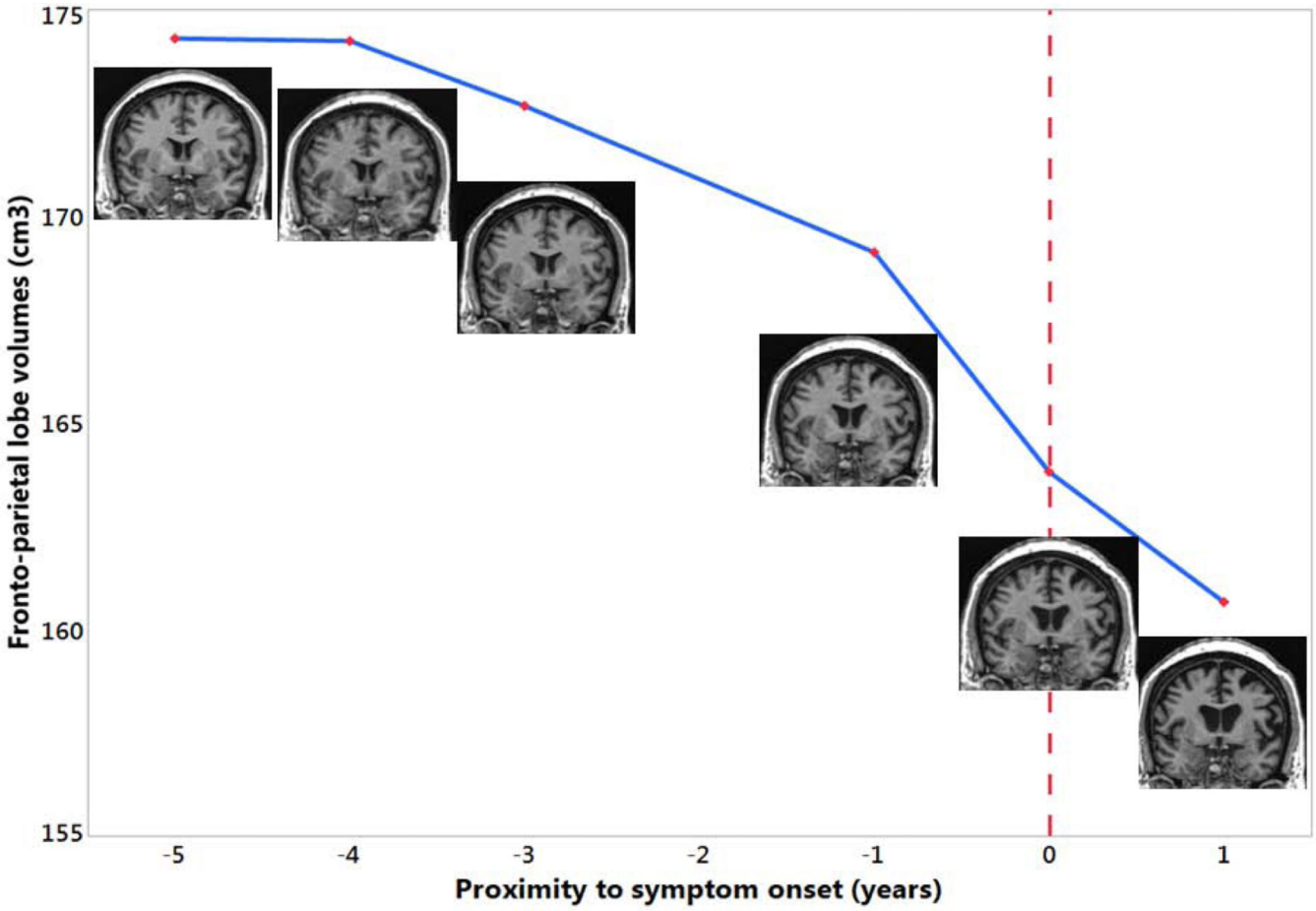

Figure 1:

Brain MRIs (coronal T1-weighted images) of one *GRN* mutation carriers who progressed from the asymptomatic to the symptomatic stage are shown in the timeline with proximity to symptom onset against the combined fronto-parietal lobe volume. 0 indicates the actual symptom onset time point. This is a female *GRN* mutation carrier who was diagnosed as behavior type of mild cognitive impairment at age 53 and progressed to bvFTD one year later. The fronto-parietal lobe volume started to decline years before symptom onset and progressively deteriorated.

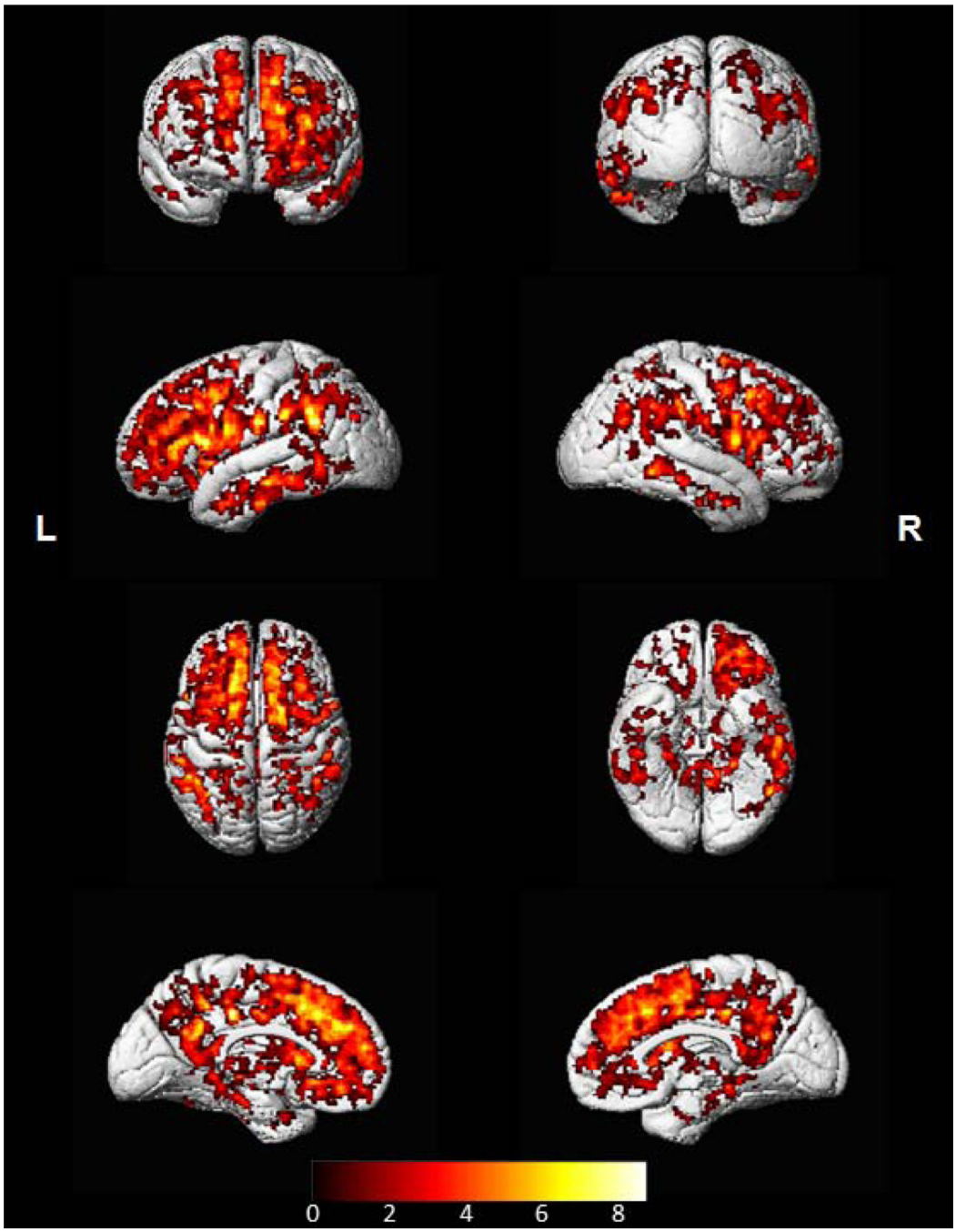

Figure 2:

Lobar cortical volumes plotted against age at MRI.

The observed trajectories are plotted in the top panel; each line shows the repeated measures for one individual in the raw data. The predicted volumes for ages 50–70 from the mixed models are plotted in the bottom panel. The lines come from the models in Table 2; each shows what we would expect per group in the age range. The blue line represents the asymptomatic *GRN* mutation carriers; the red line represents the symptomatic *GRN* mutation carriers; the black line represents the non-carriers.

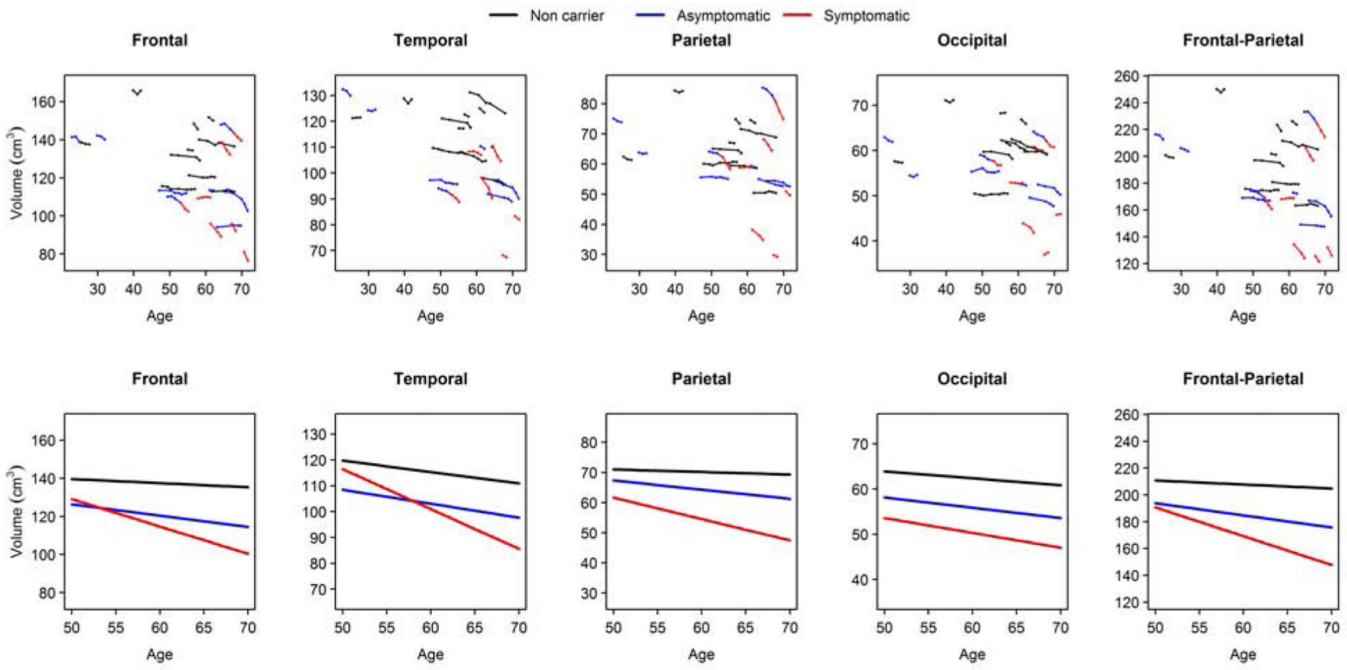

Figure 3.

Voxel-based analyses showed greater annualized rates of cortical atrophy in symptomatic *GRN* mutation carriers compared to non-carriers. The results are shown at $p<0.05$ after using the false discovery rate (FDR) correction for multiple comparisons.

Table 1:

Baseline characteristics of participants and lobar cortical volumes

	Non carrier (N = 10)	Asymptomatic (N = 8)	Symptomatic (N = 5)	P-values
No. female, n (%)	3 (30%)	4 (50%)	4 (80%)	0.58
Education, yr	15 (3) [12,20]	16 (3) [12,19]	15 (1) [14,16]	0.61
Age at MRI scan, yr	51 (11) [26,62]	50 (16) [23,65]	64 (5) [58,71]	0.10
MoCA	27 (3) [20,30]	28 (0) [27,28]	21 (6) [11,27]	<0.001*
CDR-SUM*	0.1 (0.2) [0.0,0.5]	0.0 (0.0) [0.0,0.0]	2.2 (1.9) [0.0,4.5]	<0.001*
No. MRI scans	4 [2,7]	4 [2,6]	3 [2,4]	0.51
Follow-up, yr	4.8 [1.1,9.8]	4.1 [1.0,7.5]	2.1 [1.0,3.4]	0.21
Baseline GM volume (cm^3)				
Frontal lobe	149 (17) [122,178]	136 (17) [113,157]	115 (21) [90,148]	<0.001*
Temporal lobe	131 (11) [110,148]	122 (19) [101,154]	114 (11) [97,124]	0.20
Parietal lobe	72 (9) [54,87]	67 (10) [57,86]	56 (13) [42,72]	0.01*
Occipital lobe	67 (5) [61,77]	61 (6) [54,70]	57 (7) [50,69]	0.001*

Data shown are n (%) or mean (standard deviation) or [range].

*P-values are from mixed models adjusting for age at MRI, also accounting for within-family correlations, followed by Tukey contrasts for pair-wise comparisons.

Abbreviations: MRI = Magnetic resonance image; MoCA = Montreal cognitive assessment; CDR® = Clinical Dementia Rating®; NACC = National Alzheimer's Coordinating Center; FTLD = Frontotemporal Lobar Degeneration; SB = Sum of the Boxes; TBM = Tensor based morphometry; SyN = Symmetric diffeomorphic image normalization method; CI = confidence interval.

Table 2:

Predicted annual change in lobar volumes from mixed effects models with non-carriers as the reference group.

	Frontal	Temporal	Parietal	Occipital	Frontal-Parietal
	Estimates (95% CI)	**Estimates (95% CI)**	**Estimates (95% CI)**	**Estimates (95% CI)**	**Estimates (95% CI)**
Intercept	150 (133, 168) ***	142 (132, 152) ***	75.3 (64.8, 85.7) ***	71.6 (65.3, 77.9) ***	226 (200, 252) ***
Age at MRI scan	−0.21 (−0.39, −0.04) *	−0.44 (−0.57, −0.31) ***	−0.09 (−0.17, 0.004)	−0.15 (−0.22, −0.09) ***	−0.30 (−0.54, −0.06) *
Asymptomatic	5.74 (−15.8, 27.3)	−6.38 (−22.9, 10.2)	7.28 (−5.39, 19.95)	−2.12 (−10.3, 6.10)	13.1 (−18.4, 44.7)
Symptomatic	50.7 (−2.13, 103.5)	51.9 (13.5, 90.3) *	21.9 (−5.73, 49.5)	−1.54 (−20.3, 17.2)	72.5 (−0.77, 146)
Asymptomatic × Age at MRI scan	−0.38 (−0.68, −0.08) *	−0.10 (−0.32, 0.13)	−0.22 (−0.37, −0.06) **	−0.07 (−0.18, 0.03)	−0.60 (−1.02, −0.19) **
Symptomatic × Age at MRI scan	−1.23 (−1.96, −0.49) **	−1.10 (−1.63, −0.58) ***	−0.63 (−0.99, −0.26) **	−0.18 (−0.43, 0.08)	−1.85 (−2.85, −0.85) ***

* p<0.05

** p<0.01

*** p<0.001; CI = confidence interval. The “Asymptomatic” variable was coded as 1 for asymptomatic and 0 otherwise. The “Symptomatic” variable was coded as 1 for symptomatic and 0 otherwise. If both “Asymptomatic” and “Symptomatic” are 0, then the individual comes from the non-carrier group. The non-carrier group thus functions as the reference group, so that the estimates for asymptomatic and symptomatic compare each group to the non-carrier group. These models produce the predicted lines in Figure 1. For any model where age and group appear in an interaction, estimates for the nested terms (e.g. Asymptomatic and Age are nested within “Asymptomatic × Age”) are not directly interpretable.